Vacuum Phonon Tunneling

Igor Altfeder,* Andrey A. Voevodin, and Ajit K. Roy

Thermal Sciences and Materials Branch, Materials and Manufacturing Directorate, Air Force Research Laboratory, Wright Patterson AFB, Ohio 45433, USA

(Received 7 May 2010; published 11 October 2010)

Field-induced phonon tunneling, a previously unknown mechanism of interfacial thermal transport, has been revealed by ultrahigh vacuum inelastic scanning tunneling microscopy (STM). Using thermally broadened Fermi-Dirac distribution in the STM tip as *in situ* atomic-scale thermometer we found that thermal vibrations of the last tip atom are effectively transmitted to sample surface despite few angstroms wide vacuum gap. We show that phonon tunneling is driven by interfacial electric field and thermally vibrating image charges, and its rate is enhanced by surface electron-phonon interaction.

DOI: 10.1103/PhysRevLett.105.166101 PACS numbers: 68.35.Ja, 44.40.+a, 68.37.Ef

Although temperature, one of the most fundamental categories in physics, can be traditionally defined only for macroscopic systems [1], the advances of nanoscale instrumentation [2], ultraclean vacuum technologies [3], and research of individual nanostructures [4,5] have enabled the extension of this term down to atomic scale, and the actual experimental ability to define or measure the temperature at the level of individual atoms. For example, scanning tunneling microscopy (STM) experiments have shown that an individual adatom on a surface loses its kinetic energy and becomes immobilized when cooled to low temperatures, which allows manipulating this adatom using local electric field of STM tip [3]. Another interesting example of nanometer scale thermal phenomena is the temperature and the heat transfer at the end of STM tip [6–8], which is usually an atomically sharp asperity. Since tunneling electrons always choose the shortest path, it is the temperature of the last tip atom which actually determines the thermal energy broadening of the tunneling current. Understanding basic thermal phenomena at atomic and nanometer scale is crucial for achieving success in such fields as thermoelectric materials, interfacial transport, and design of molecular electronic circuits.

In this Letter, we show that the temperature of the terminating atom of STM tip can be directly established using inelastic electron tunneling spectroscopy. Moreover, our study revealed the phenomenon of vacuum phonon tunneling, transmission of tip thermal vibrations towards sample surface through few angstrom wide vacuum gap. To explain the phenomenon of phonon tunneling, we propose a model of thermally vibrating image charge, ''thermal mirage.'' By comparing experimental data and theory, we show that the thermal energy transmitted through atomically narrow vacuum gap due to thermal vibration of image charges exceeds, by 10 orders of magnitude, the blackbody thermal radiation energy. The result has important implications for thermal transport at heterointerfaces both on micro- and on macroscale.

For our experiments we used ultrahigh vacuum (UHV) variable-temperature STM, a frequently used experimental setup which allows cooling the sample to low temperatures, although the tip always stays hot (~ 275 K) [9]. Motivated by theoretical predictions of near-field enhanced radiative heat transport [7,8], it was recently shown, also using such an experimental setup, that a lithographically fabricated thermocouple placed a few microns apart from the end of the tip cools by ~ 1 K when the tip is located in the vicinity of a cold sample surface [6]. Because in this geometry the highest temperature gradient is anticipated at the very end of the STM tip, we, instead, use inelastic electron tunneling spectroscopy (IETS) [10] as *in situ* atomic-scale thermometer. Since pioneering IETS work it has been established that the effective width of phonon peaks is limited by thermally broadened Fermi-Dirac distribution [10,11], and the resonance full width at half maximum (FWHM) $\approx 5.4k_BT$. One can show that in the experimental situation of interest, i.e., when tunneling electrodes may have different temperatures, the thermal broadening of phonon resonances will be determined by the average temperature of electrodes: FWHM $\approx 5.4k_B\bar{T}$ [12]. As we stated earlier, for atomically sharp STM tip the thermal vibration spectra of its last atom determines the energy broadening of tunneling current and the width of experimentally observed phonon resonances, and therefore the temperature of this atom can be directly measured using STM-IETS. A novelty of this experimental method requires a special comment: previously published STM-IETS works [13–17] were made using isothermal setups, where tip temperature = sample temperature and the experimental study of atomic-scale thermal transport was not possible.

The sample for our study was Au(111) film on mica, which we annealed in UHV to 400 °C to clean its surface. The STM tip was electrochemically etched 100 μm diameter Pt/Ir wire, which was also cleaned by UHV annealing using the electron beam technique. The atomic level cleanness of the tip and sample surfaces has been confirmed by (a) STM observation of Au(111) atomic lattice (inset in Fig. 1) and (b) the observation of exponential tunneling current vs vacuum gap width dependence (lower inset in Fig. 4). The base pressure in the UHV

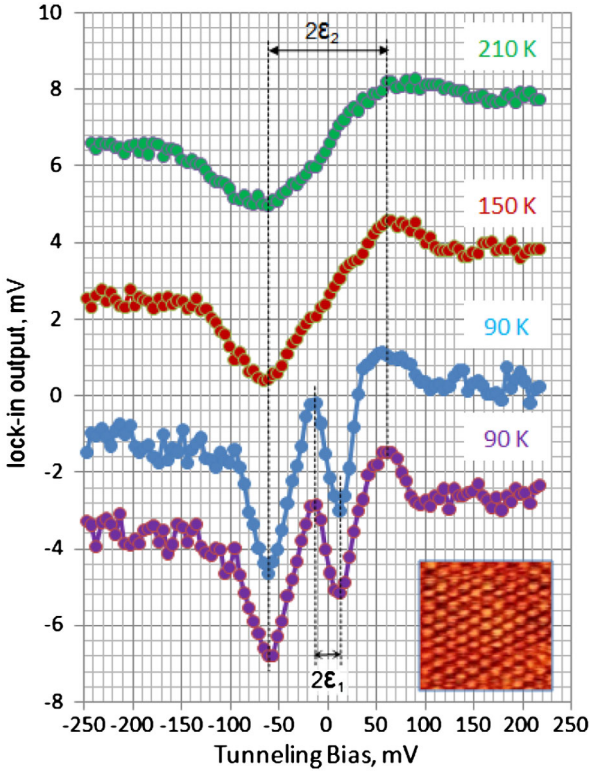

FIG. 1 (color online). Inelastic tunneling spectra obtained on Au(111) surface at three different sample temperatures: 210 K (upper curve), 150 K (middle curve), and 90 K (two lower curves: obtained at different portions of sample surface). The curves are offset along the vertical axis. Inset: 3×3 nm^2 atomically resolved STM image of Au(111) sample. Obtained at 90 mV sample bias and 0.5 nA current.

STM system (model UHV-3000 from RHK Technology) was 4.5×10^{-11} Torr. The sample temperature was measured *in situ* using *K*-type thermocouple attached to the front surface. For IETS measurements we used 5 mV sample bias modulation amplitude ($V_{\mathrm{rms}} = 3.5$ mV) at a frequency of 1500 Hz and lock-in detection at second harmonic in order to obtain d^2I/dV^2 representing the phonon density of states (DOS) [18]. Because measurements of phonon density of states require the accumulation of signals during large periods of time, ~1 hour per spectra in our case, the measurements were made at relatively large tunneling conductance in order to maximize the signal-to-noise ratio. The independence of the tip temperature on the sample temperature has been shown in Ref. [9] describing a variable-temperature design, whose commercial copy we used for our experiments. The spectra were analyzed by Gaussian fitting [14], and $\bar{T}$ was determined from equation [11,12]: $\mathrm{FWHM} = \sqrt{(5.4k_B\bar{T})^2 + (1.7eV_{\mathrm{rms}})^2}$.

In Fig. 1 we show IETS spectra obtained on a clean Au(111) surface at three different sample temperatures: 90 K (two lower curves in Fig. 1), 150 K (middle curve in Fig. 1), and 210 K (upper curve in Fig. 1). The measurements were made at 10 MΩ tunneling gap resistance, which corresponds to 3 Å vacuum separation between the STM tip and the sample surface. Tunnel *I*-*V* characteristics (not shown), recorded simultaneously with d^2I/dV^2 spectra, were linear and featureless with current changing within ±25 nA. At 90 K, two symmetric low-energy features appear in IETS spectra separated from each other by $2\varepsilon_1 = 24$ mV. These resonances were previously observed on face-centered cubic (fcc) and hexagonal close-packed (hcp) surface regions of Au(111) [15] and associated with inelastic phonon emission peaks. Indeed, their energy $\varepsilon_1 = 12$ meV is close to bulk Debye temperature of Au $\Theta = 165$ K. The higher energy features in IETS spectra at $\pm\varepsilon_2$ ($\varepsilon_2 = 60$ mV) represent phonon emission-reabsorption dips, not characteristic of Au(111) surface [15], and therefore associated with STM tip [19,20]. In previous spectroscopic surface studies, including Raman and infrared (IR) spectroscopy, very similar frequencies, 470–500 cm^{-1}, have been attributed to vibration of Pt-C [21] bond due to adsorption of CO molecules on the Pt surface [22]. We conclude that the tip apex is terminated by a CO molecule. When the sample temperature has been raised to 150 K (see the middle curve in Fig. 1) the low-energy $\pm\varepsilon_1$ spectral features disappeared. The high-energy IETS features remain visible in this spectrum, though these features appear to be broader than on the lower curves in Fig. 1. Upon further increase of the sample temperature to 210 K (see the upper curve in Fig. 1) the additional broadening of IETS dips takes place. The disappearance of closely spaced $\pm\varepsilon_1$ features at higher sample temperatures most likely has to do with their thermal broadening and further enhanced by their mutual overlapping [23]. In Fig. 2 we show the temperature-dependent phonon density of states obtained from Fig. 1 data by averaging the contributions for positive and negative tunnel bias, using

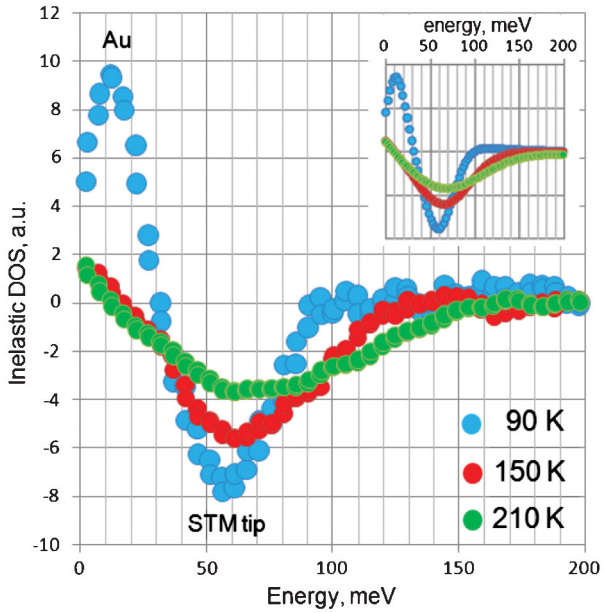

FIG. 2 (color). Temperature-dependent IETS density of states obtained from spectra in Fig. 1 by averaging the contributions for positive and negative tunnel bias. Inset: Gaussian fit curves.

antisymmetric function $f(-V) - f(V)$. Very surprisingly, for tip-induced $\pm\varepsilon_2$ features the effective temperatures determined from spectral FWHM: $\mathrm{FWHM}_{90\ \mathrm{K}} = 40 \pm 5$ mV ($\bar{T} = 85 \pm 10$ K), $\mathrm{FWHM}_{150\ \mathrm{K}} = 76 \pm 7$ mV ($\bar{T} = 161 \pm 15$ K), $\mathrm{FWHM}_{210\ \mathrm{K}} = 97 \pm 7$ mV ($\bar{T} = 206 \pm 15$ K) essentially coincide with sample temperatures. Thus, our measurements show that the terminating atom of the STM tip remains in thermal equilibrium with sample surface despite a 3 Å wide vacuum gap separating this atom from the cold surface. We would like to notice that for a "hot" STM tip the experimental observation of phonon resonances would not be possible at all: because of its thermally broadened Fermi level the corresponding spectral FWHM would be equal to 100 mV (at 90 K), 107 mV (at 150 K), and 120 mV (at 210 K).

Because of the considerable amount of time required for IETS measurements and unavoidable for VT-STM thermal drift, the resonant spectra of Au(111) surface ($\pm\varepsilon_1$ features) represent the averaged over few nm^2 rather than site-selective, as in Ref. [15], information. The spectral width of this resonance requires a special discussion. The analysis shows that the $\pm\varepsilon_1$ feature at 90 K is characterized by FWHM $= 24 \pm 2$ mV rather than 40 mV. This may be due to the strong electron-phonon interaction (EPI) characteristic of 2D systems [24], such as Au(111) surface. Because of strong 2D EPI, the surface resonance possesses both phononic and electronic components, and the later is being primarily picked up by STM measurements. Its thermal broadening is $3.5k_BT$, i.e., by a factor of 1.5 less than what would be for week EPI. As we shall show later in the manuscript, strong surface EPI plays important role in cooling the tip apex to cryogenic temperatures.

Although the issue of heat exchange between the STM tip and cold sample surface has been actively debated in the literature [6–8], our conclusion that the last tip atom equilibrates its temperature with sample surface is rather unexpected. It seemingly contradicts to an intuitive estimation that the energy exchange through vacuum cannot exceed the solid state heat conductance, mainly electronic heat conductance for metallic STM tip. In the discussion part of the manuscript, we will show that it is the local electric field of the STM tip which causes strong coupling between tip and sample surface lattice vibrations and results in an unexpected increase of heat flux through thin vacuum gap, exceeding by 10 orders of magnitude the prediction of blackbody radiation theory and by nearly 6 orders of magnitude the state-of-the-art theory predictions [8] for near-field radiative heat transport.

At low tip-sample biases, which we used for measuring IETS spectra, the electric field of the STM tip is mainly caused by work-functions difference ($\Delta\Phi_{\mathrm{Au/Pt}} \approx -0.7$ eV): $\mathbf{E} = \Delta\Phi/d$, where $d \approx a$ is the vacuum gap width (a- interatomic distance). Although the classical "image charge" induced by this field is supposed to be located at a distance of $-d$ beneath the surface (see Fig. 3), the actual screening cloud in the interfacial double-charged layer is located on the sample surface and is represented by an exchange hole [25] whose radius $\approx d$. As we show in Fig. 3, due to electric field thermal vibrations of the tip apex are transmitted to the sample surface as forced thermal vibrations of image charge and exchange hole. This happens because the vibration frequency of STM tip, $\hbar\omega \approx 60$ meV, is much less than Au(111) surface plasmon frequency [26] (including short-wavelength acoustic plasmons [27,28]) and the image charge has sufficient time to follow the local electric field of the tip. Modeling the emission of phonons from this thermally vibrating surface charge as from the surface "hot spot" [29] yields the following expression for energy loss:

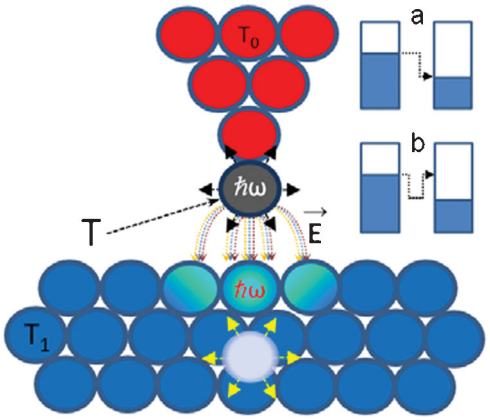

FIG. 3 (color). Screening charges induced on sample surface by local electric field of STM tip. Vibration of tip apex changes the spatial position of the field maximum. Thermal vibrations of the STM tip are transmitted to sample surface as forced "thermal" vibrations of screening charges. Inset: energy diagrams for tip-sample inelastic tunneling processes: (a) phonon emission, (b) resonant emission-reabsorption.

$$P_{\mathrm{ph}} = A\varepsilon_{\mathrm{ph}}\frac{\pi^2 k_B^2}{60\hbar^3 v_s^2}(T^4 - T_1^4), \qquad (1)$$

where A is the hot spot area, v_s—sound velocity, $\varepsilon_{\mathrm{ph}}$—phonon emissivity of the hot spot, and (T, T_1) are the tip apex and the sample temperatures, respectively. Under the experimental conditions relevant to this Letter: $d \approx a$, $A \approx \pi a^2$, the charge density in the surface exchange hole achieves its maximum value [25], and we can assume $\varepsilon_{\mathrm{ph}} \approx 1$. Physically, Eq. (1) implies that the atomically compact vibrating charge cloud, located right under the tip, couples through Coulomb potential to a nearest surface atom and forces it to vibrate with amplitude comparable to the vibration amplitude of a tip. An important role in this process belongs to strong surface EPI, which was discussed earlier. In equilibrium, the phonon emission term (1) must be balanced by thermal energy delivered to the tip apex through solid state conductance. The later can be found from the Wiedemann-Franz law suggesting that thermal conductance of the atomically sharp tip represents the product of electrical conductance quantum [30] ($2e^2/h$), Lorentz number ($\pi^2 k_B^2/3e^2$) and temperature, giving rise

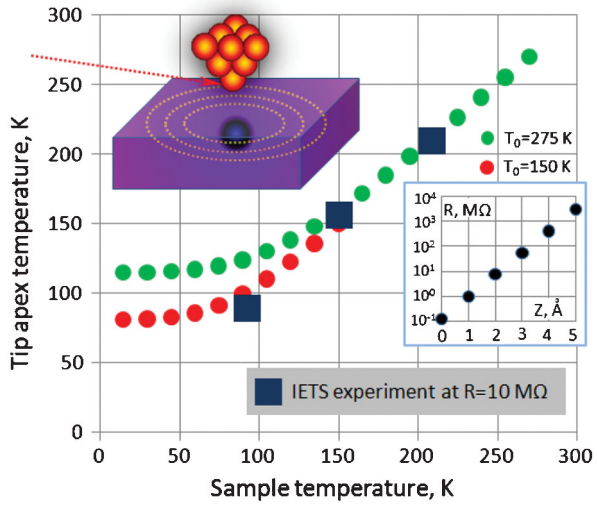

FIG. 4 (color). The dependence between STM tip apex temperature and sample temperature predicted by model of "thermal mirage." Green and red curves correspond to tip "bulk" temperatures of 275 and 150 K, respectively. Inset: the dependence of vacuum gap resistance on tip vertical displacement for the Au(111) sample. The IETS measurements were made at 10 MΩ resistance.

to an expression $\pi k_B^2 T/3\hbar$: a (spin) factor of 2 multiplied quantum of thermal conductance [31]. Therefore, thermal energy delivered to the tip apex [7,8] equals to

$$P_{\rm tc} = \frac{\pi k_B^2}{6\hbar}(T_0^2 - T^2), \tag{2}$$

where T_0 is the temperature of the tip "bulk," i.e., the Pt asperity holding the terminating tip atom. Now the expression for energy balance, $P_{\rm tc} = P_{\rm ph}$, takes the following simple form:

$$\frac{\pi^4}{10}\frac{T^4 - T_1^4}{\Theta^2} = T_0^2 - T^2, \tag{3}$$

where $\Theta = \pi\hbar v_s/a$ is Debye temperature of the sample. The dependence between tip apex temperature and sample temperature is shown in Fig. 4 for $\Theta = 165$ K and $T_0 = 275$ or 150 K (green vs red curve). Because it was earlier established that the tip cooling may occur not only at the very end [6] the modeling was done at two different T_0. The dependence is essentially linear with the tendency towards saturation at very low sample temperatures: STM equivalent of low-temperature Kapitza resistance. The experimental data obtained from IETS spectra are shown on top of model curves. The comparison of model Eq. (1) with experimental data clearly shows that field-induced phonon tunneling represents the most likely mechanism of thermalization between atomically sharp STM tip and cold sample surface.

In conclusion, we demonstrate that the temperature of the terminating atom of STM tip can be determined using the innovative technique of UHV variable-temperature inelastic electron tunneling spectroscopy. By advancing the understanding level of atomic-scale thermal phenomena, our result, at the same time, has important implications for thermal transport at macroscopic hetero-interfaces where nanoasperities often play a crucial role. We show that field-induced thermal transport through the atomically thin interfacial gap can exceed the Planck's radiation energy by a factor of $c^2/v_s^2 \sim 10^{10}$.

The authors thank S. Patton, K. Matveev, M. Kozlov, Y. Bazaliy, P. Hagelstein, A. Kittel, M. Bode, and A. Balatsky for interesting discussions. The research was supported by AFOSR.

*Igor.Altfeder.ctr@wpafb.af.mil

[1] L. D. Landau and E. M. Lifshitz, *Statistical Physics* (Pergamon Press, Oxford, 1980), Pt. 1.
[2] G. Binnig *et al.*, Phys. Rev. Lett. **49**, 57 (1982).
[3] D. M. Eigler and E. K. Schweizer, Nature (London) **344**, 524 (1990).
[4] L. Bartels *et al.*, Science **305**, 648 (2004).
[5] R. D'Agosta, N. Sai, and M. Di Ventra, Nano Lett. **6**, 2935 (2006).
[6] A. Kittel *et al.*, Phys. Rev. Lett. **95**, 224301 (2005).
[7] J. B. Pendry, J. Phys. Condens. Matter **11**, 6621 (1999).
[8] A. I. Volokitin and B. N. J. Persson, Rev. Mod. Phys. **79**, 1291 (2007).
[9] Q. Dai *et al.*, Rev. Sci. Instrum. **66**, 5266 (1995).
[10] J. Lambe and R. C. Jaklevic, Phys. Rev. **165**, 821 (1968).
[11] J. Klein *et al.*, Phys. Rev. B **7**, 2336 (1973).
[12] From the empirical rule of additions, frequently used in IETS, we find $\bar{T} \approx \sqrt{(T_{\rm tip}^2 + T_{\rm sample}^2)/2}$.
[13] B. C. Stipe, M. A. Rezaei, and W. Ho, Science **280**, 1732 (1998).
[14] J. R. Hahn, H. J. Lee, and W. Ho, Phys. Rev. Lett. **85**, 1914 (2000).
[15] H. Gawronski, M. Mehlhorn, and K. Morgenstern, Science **319**, 930 (2008).
[16] M. Grobis *et al.*, Phys. Rev. Lett. **94**, 136802 (2005).
[17] L. Vitali *et al.*, Phys. Rev. Lett. **93**, 136103 (2004).
[18] At zero phase shift the second harmonic lock-in detection yields $-d^2I/dV^2$.
[19] B. N. J. Persson and A. Baratoff, Phys. Rev. Lett. **59**, 339 (1987).
[20] L. Vitali *et al.*, Phys. Rev. B **81**, 153409 (2010).
[21] G. Bylholder and R. Sheets, J. Phys. Chem. **74**, 4335 (1970).
[22] L. Maya and E. W. Hagaman, J. Phys. Chem. B **102**, 1951 (1998).
[23] W. Wang *et al.*, Nano Lett. **4**, 643 (2004).
[24] Ph. Hofmann *et al.*, New J. Phys. **11**, 125005 (2009).
[25] V. Sahni and K.-P. Bohnen, Phys. Rev. B **31**, 7651 (1985).
[26] S. J. Park and R. E. Palmer, Phys. Rev. Lett. **102**, 216805 (2009).
[27] Diaconescu *et al.*, Nature (London) **448**, 57 (2007).
[28] V. M. Silkin *et al.*, Phys. Rev. B **72**, 115435 (2005).
[29] J. P. Wolfe, *Imaging Phonons: Acoustic Wave Propagation in Solids* (Cambridge University Press, New York, 1998), p. 83.
[30] L. Olesen *et al.*, Phys. Rev. Lett. **72**, 2251 (1994).
[31] K. Schwab *et al.*, Nature (London) **404**, 974 (2000).